

Research Paper

Effect of sampling density and location on airflow rate measurements in a naturally ventilated pig barn with an outdoor exercise yard: A boundary layer wind tunnel study



Xuefei Wu ^a, Sabrina Hempel ^a, David Janke ^a, Barbara Amon ^{b,c}, Guoqiang Zhang ^d, Jürgen Zentek ^e, Thomas Amon ^{a,f}, Qianying Yi ^{a,*}

^a Department of Sensors and Modelling, Leibniz Institute for Agricultural Engineering and Bioeconomy (ATB), Max-Eyth-Allee 100, 14469, Potsdam, Germany

^b Department of Technology Assessment, Leibniz Institute for Agricultural Engineering and Bioeconomy (ATB), Max-Eyth-Allee 100, 14469, Potsdam, Germany

^c University of Zielona Góra, Faculty of Civil Engineering, Architecture and Environmental Engineering, Zielona Góra, Poland

^d Department of Civil and Architectural Engineering, Aarhus University, Inge Lehmanns Gade 10, Aarhus, 8000, Denmark

^e Institute of Animal Nutrition, Freie Universität Berlin, Königin-Luise-Straße 49, 14195, Berlin, Germany

^f Institute for Animal Hygiene and Environmental Health (ITU), Free University Berlin, Robert-von-Ostertag-Str. 7-13, 14163, Berlin, Germany

ARTICLE INFO

Keywords:

Natural ventilation
Laser Doppler anemometer
Pig housing system
Outdoor yard
Animal welfare

ABSTRACT

An accurate ventilation rate estimation is the basis for developing ventilation strategies, optimising indoor air quality and determining pollutant emissions from livestock buildings. To accurately quantify the airflow rate of a novel naturally ventilated pig barn with an outdoor exercise yard, the influence of sampling density and location on the airflow rate measurement was studied. The experiment was conducted in a large atmospheric boundary layer wind tunnel by measuring the airflow velocity at the openings (the yard opening and the window of the indoor room) of a scaled pig barn model. Under four wind directions (0° , 60° , 120° , and 180°), the study evaluated four sampling densities distributed separately along the vertical or the lateral directions of the opening, different mesh-like sampling strategies, and airflow rate measurement with or without considering the edge effects of the opening. The results showed that: 1) Sampling densities distributed vertically and laterally along the yard opening, as well as those distributed vertically along the window, were significantly affected by wind directions ($p < 0.05$). 2) The mesh-like sampling strategy can ensure accurate measurement results with a difference ratio of less than 5 %. 3) Suitable sampling densities without considering the wall effect caused by the vertical edge of the opening can still support reliable airflow rate measurement. The results of this study contribute to developing the direct method of airflow rate measurements in naturally ventilated livestock buildings.

Nomenclature table

ANOVA	Analysis of Variance
BL	Baseline configuration
CV	Coefficient of variation
DR	Difference ratio or the change ratio
LDA	Laser Doppler Anemometer
P, P_{BL}	A placeholder, and baseline property
2D, 3D	Two-dimensional, three-dimensional
A^* , A_w , A_L	An effective opening area (m^2), the windward and leeward opening area (m^2)
α	Wind direction ($^\circ$)
C_d	Discharge coefficient of the opening

(continued on next column)

(continued)

$E_{u,red}$	Spectral distribution of the turbulent kinetic energy
f_{red}	Reduced frequency
Q , Q^*	Airflow rate ($m^3 s^{-1}$), the normalised airflow rate
σ , \bar{u}	Standard deviation, the mean velocity ($m s^{-1}$)
u , v , w	Along-wind, crosswind, and vertical component of wind ($m s^{-1}$)
u_∞ , u_{ref}	Free stream velocity ($m s^{-1}$), the reference airspeed ($m s^{-1}$)
u_z	Along-wind velocity component at a height ($m s^{-1}$)
z , z_0	Measured height (m), a roughness length (m)

* Corresponding author.

E-mail address: QYi@atb-potsdam.de (Q. Yi).

1. Introduction

A novel type of livestock building, naturally ventilated pig barns with outdoor exercise yards, where the exercise yard provides space for pigs to play and excrete and the indoor area serves as a resting and feeding space, is a promising housing design to improve animal welfare. This is because the separation of excretion and resting area follows the pigs' natural behaviours, and the presence of the yard can increase area for movement and also provide pigs with more contact with fresh air and sunlight. Furthermore, the excretion could primarily occur in the yard, consequently improving the management of manure and reducing fouling of the animals and the indoor area (Andersen et al., 2020). To guarantee the fulfilment of those design goals of this type of pig barn, a good ventilation system is required. The airflow rate, which is directly related to the exchange of fresh air and the gas emissions, is one of the key factors for evaluating the ventilation system (Kiwan et al., 2013; Seedorf et al., 1998). To get the accurate airflow rate measurement, there have been many studies (Cao et al., 2023; Janke, Yi, et al., 2020; Samer et al., 2011, 2012). Those studies are based on the conventional barns, which are not equipped with an outdoor yard, and thus, further research is needed to accurately measure the airflow rate in barns with outdoor yards before evaluating and optimising the ventilation system of barns with outdoor yards.

The methods for quantifying the airflow rate of naturally ventilated livestock buildings mainly include indirect methods (such as tracer gas techniques, mass balance methods, and sensible heat balance methods) and the direct method (velocity measurements at the building openings). The suitability or choice of the method depends on many factors (Joo et al., 2014). Wu et al. (2025) studied the ventilation inside this kind of barn and reported the different airflow patterns between the yard and the room caused by its complicated configuration. This configuration makes it hard to achieve the assumption of uniform distribution and fully-mixed tracers. Meanwhile, different behaviours of the animals in the yard and the indoor housing area might lead to varying production of H₂O, heat and CO₂ while using the gas and sensible heat balance methods. Those factors affect the accuracy of the indirect method employed in such pig barns. The direct method requires many measurements and is therefore costly, and it cannot capture airflow information at the animal level. However, the direct method is less influenced by animal physiology and behaviour (Wang et al., 2016) and can capture the airflow rate under fluctuating wind conditions (De Vogeeler et al., 2016). Therefore, the direct method demonstrates a promising future in obtaining a stable and accurate measurement of the airflow rate for the barn with an outdoor yard.

The direct method has been used to quantify the airflow rate of naturally ventilated livestock buildings in the past. Janke, Yi, et al. (2020) reported that suitable sampling points of the direct method can result in errors of the measured airflow rate of less than 5 % for a large naturally ventilated building, but their measurements were only carried out under perpendicular wind direction. Wang et al. (2016) found the CO₂ balance method and the direct method yielded similar ventilation rates with an integration time of 24 h, while significant differences were observed with shorter integration times (1, 2, and 12 h). De Vogeeler et al. (2017) applied the direct method at the side vents of a naturally ventilated animal mock-up building, and the unsuitable sampling locations led to systematic over- or underestimation of the airflow rates. Van Overbeke, De Vogeeler, et al. (2014, 2015) and Van Overbeke, Pieters, et al. (2014) evaluated the performance of the direct method through 2D and 3D ultrasonic anemometers and then applied it in a test naturally ventilated pig house, and found that 2D ultrasonic anemometers gave rise to relatively high measurement errors while 3D ultrasonic sensors kept relative errors below 10 %. Those studies illustrate that the performance of the direct method depends on the number and location of the measurement points, which are fundamentally affected by the airflow distribution. Outside wind direction significantly affects the distribution of airflow velocities, thereby greatly influencing the

accuracy of the direct method. Increasing the number of measurement points can generally mitigate this effect, but results in higher costs for implementing the measurement systems. Wu et al. (2025) measured the airflow rate in a barn with an outdoor yard under four wind directions, using the direct method with 40 and 50 measurement points distributed at the two openings, respectively, but their study did not systematically evaluate the influence of the number and location of the measurement points. Consequently, while the use of a large number of measurement points would significantly improve accuracy, it is challenging to apply this approach on farms due to the high measurement costs and time-consuming. Therefore, evaluating the performance of the direct method under different wind directions is essential to help to minimise redundant measurements in this novel type of livestock barn under natural ventilation.

Furthermore, the obstructive presence of the opening's edges, pillars, and walls passing through the opening redistributes the surrounding airflow, leading to a decreased air velocity—a phenomenon named “wall effect” in our study. Measurements near the obstruction are mostly skipped in studies on naturally ventilated barns, treating them as airflow without obstruction when calculating the airflow rate. This assumption would lead to more uncertainties during the airflow rate measurement (Janke, Yi, et al., 2020; Van Overbeke et al., 2015). On the one hand, the measurement is suggested to be positioned as far as possible from obstacles such as beams and walls (Janke, Yi, et al., 2020). On the other hand, Van Overbeke, Pieters, et al. (2014) found the main cause of the measurement error in the airflow rate of a naturally ventilated animal house was the unaccounted edge effects of the openings although their experiment could not provide the influence of vertical and horizontal sampling measurements on the wall effect due to the sensor geometries influencing the airflow distribution. Therefore, to clarify its influence on the airflow rate measurement, it is essential to take the wall effect into account when evaluating the accuracy of the direct method for the barn with an outdoor yard.

The uncontrollable and fluctuating local climate (e.g., wind speed and direction, air temperature) makes it challenging to evaluate the accuracy of the direct method on the farm. Conversely, wind tunnels where well-controlled boundary conditions can be generated, can overcome problems caused by continuously changing outdoor environments. Meanwhile, the atmospheric boundary layer wind tunnel can simulate the wind profile above the farmland, and the results can be transferred into the natural scale with a more realistic wind profile if similarity laws are obeyed (VDI. 2024.). Therefore, the atmospheric boundary layer wind tunnel can serve as an alternative to evaluate the applicability of the direct method, and the results can provide a reliable reference for on-farm experiments (Cheng et al., 2024; Lee et al., 2004).

Above all, the objective of this study is to evaluate the accuracy of the direct method in quantifying the airflow rate of the barn with an outdoor yard based on an atmospheric boundary layer wind tunnel study, including: 1) evaluating the performance of different sampling densities in the airflow rate measurement, 2) examining the influence of wind directions on the direct method, and 3) comparing the measured airflow rate with/without capturing the influence of the opening edges on the airflow.

2. Materials and methods

2.1. Configuration of the wind tunnel and instrument

The experiment was conducted in a large atmospheric boundary layer wind tunnel, situated at Leibniz Institute for Agricultural Engineering and Bioeconomy (ATB) in Germany. This wind tunnel is specifically designed to investigate ventilation and dispersion processes in agricultural applications. Its internal dimensions are 28.5 m in length, 3.0 m in width, and 2.3 m in height. The wind tunnel consists of an inlet nozzle, a 19.5 m inflow section with roughness elements and spires, a test section where the scaled model is positioned, and an outlet section equipped

with an axial fan (Fig. 1(a)). More information on the wind tunnel model can be found in the literature (Janke, Yi, et al., 2020; Yi et al., 2018).

The free stream air velocity u_∞ was measured at the centre of the entrance to the wind tunnel using a Prandtl tube at a height of 1.3 m from the wind tunnel floor. Air velocities were measured using a 2D fibre-optic Laser Doppler anemometer (LDA) (Dantec Dynamics, Skovlunde, Denmark) mounted on a traverse system with precise probe positioning with an uncertainty of <0.1 mm (Fig. 1(b)). The wind velocity has three components: u (along-wind), v (crosswind), and w (vertical). The two-dimensional vectors (uv and uw) measured in the study were obtained by rotating the LDA probe.

2.2. Configuration of the scaled pig barn model and the wind directions

A model of a naturally ventilated pig barn with an outdoor exercise yard was built in 1:50 scale, based on a prototype pig barn located in Wehnen, Germany ($53^{\circ}10'20.5''\text{N}$ $8^{\circ}07'26.4''\text{E}$) (Fig. 2(a)). The scaled model was made of 3 mm thick acrylic glass.

A partition wall in the middle of the barn (Mid-Partition wall in Fig. 2(b)) divides the barn into two identical sections, referred to as Compartment 1 and Compartment 2 (abbreviated as Comp.1 and Comp.2). Each compartment contains four pens, with each pen having one cubicle designed for pigs to sleep inside (Fig. 2(b)), and the cubicle has a maximum height of 24 mm at the maximum open position during the experiment. The barn includes an exercise yard (exercise area) directly attached to a room (indoor area). The wind flowing between the yard and the room goes through Mid-opening in Fig. 2(c), and the pigs access those two regions through the doors embedded in the wall under Mid-opening. These doors are typically kept closed but can be opened by the pigs, so they were not included in the scaled model. It is a solid wall below Mid-opening in Fig. 2(c). The scaled model does not include a ridge opening, and it is also a solid wall above Mid-opening shown in Fig. 2(c). The presence of cows (without considering heat production) was reported to have an insignificant impact on the flow inside a naturally ventilated cattle barn under perpendicular wind direction to the ventilation openings (Nosek et al., 2020). Therefore, considering the smaller size of pigs compared to cattle and the relatively lower stocking densities in the barn with an outdoor yard compared to conventional pig barns, along with the minor influence of small structures (e.g., feeding and drinking devices, internal partitions) on airflow rate measurements, these elements were not considered in the model construction.

The airflow rate measurements were performed at two openings of the scaled model, and they are: The window, which is referred as Window in this study, located on the side wall of the room and kept fully

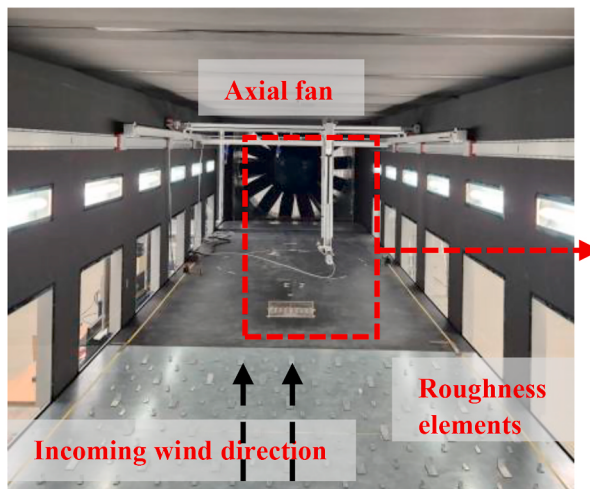
open (20 mm high in the scaled model) during the experiment; The yard opening in the exercise yard with a fixed opening height of 58 mm high, referred as Yard Opening in this study. Those two openings had a lateral opening length of 421 mm. Since the Mid-Partition wall separates Comp.1 and Comp.2, there is a wall in the middle of those openings, seen from the vertical blue line in the middle of the openings in Fig. 2(c).

To evaluate the influence of wind direction on sampling density and location, four wind directions at 60° intervals, i.e., $\alpha = 0^\circ, 60^\circ, 120^\circ$, and 180° , were considered (Fig. 2(d)). These directions were achieved by manually adjusting the orientation of the scaled model relative to the incoming wind in the wind tunnel. For all four model orientations, the maximum blockage ratio was 3.2 %, well below the recommended maximum of 5 % for wind tunnel experiments (VDI-VereinDeutscher, 2024).

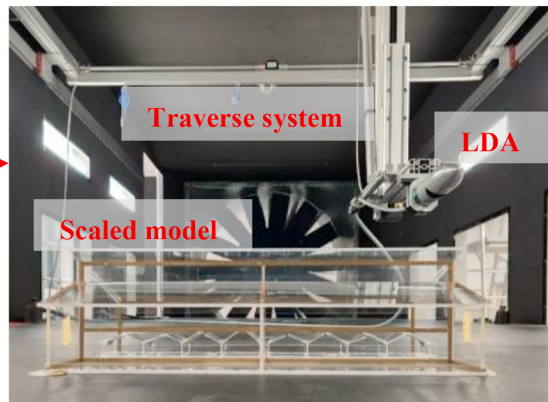
2.3. Approach-flow profiles

To ensure fully-developed turbulent flow through the opening, which confirms the results could be scaled up to the natural environment, a Reynolds number independence test was conducted at free stream velocities $u_\infty = 3.0, 4.0, 6.0, 8.0, 10.0, 12.0$, and 14.0 m s^{-1} under wind incidence angles of $\alpha = 0^\circ, 60^\circ, 120^\circ$, and 180° . Measurements were conducted inside the room (point C) at vertical intervals of 10 mm, ranging from 20 mm to 110 mm above the model floor, with a distance of 23 mm to Mid-opening. The results indicated that when the free stream velocities u_∞ were over 10.0 m s^{-1} , the airflow patterns inside the model did not change with a further increase in wind speed, indicating that the Reynolds number independence was achieved. More details on the Reynolds number independence test can be found in the paper (Wu et al., 2025). Therefore, $u_\infty = 10.0 \text{ m s}^{-1}$ was ultimately selected for subsequent wind tunnel measurements in this study.

To ensure the quality of the simulated approaching flow, a stability test of the wind profile was conducted under a free stream velocity of 10.0 m s^{-1} . The wind profile was measured along two lines located at the windward lateral edges of the region, with measurement points positioned at heights ranging from 13 mm to 603 mm above the wind tunnel floor (points A and B in Fig. 2(d)). Along these two lines, the u -component exhibited a maximum difference of 1.01 % in the value of turbulence intensity and a maximum relative difference of 3.2 % in velocity, compared to the average values at each measurement point (as shown in Fig. 3(a) and (b)). The wind profile under a free stream velocity $u_\infty = 10.0 \text{ m s}^{-1}$ without the model was measured along those two measurement lines as well. A logarithmic vertical velocity profile was obtained through regression (Fig. 3 (a)), as shown in equation (1):



a. Picture of the wind tunnel with model inside



b. LDA above the scaled model

Fig. 1. Configuration of the atmospheric boundary layer wind tunnel (The dashed arrow does not represent a physical entity and is intended solely for illustrative purposes).

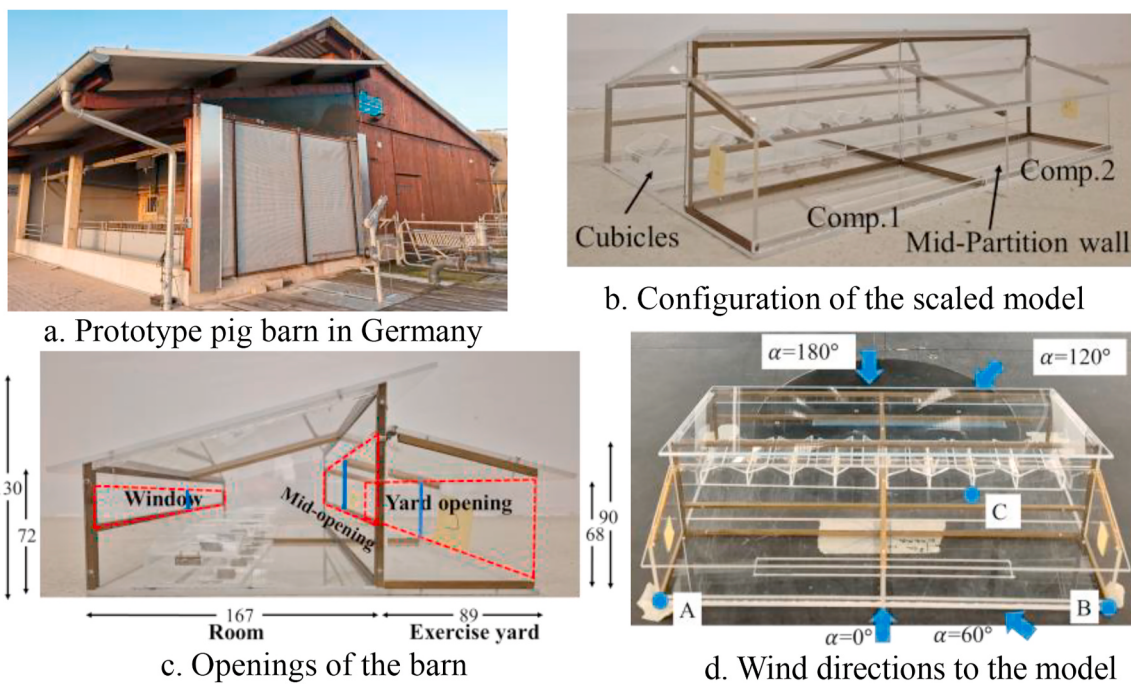


Fig. 2. Prototype pig barn and configuration of the 1:50 scaled model of the pig barn and its wind directions (unit: mm). Comp. 1 and Comp. 2 represent compartments 1 and 2 of the scaled model. Blue arrows indicate the incoming wind directions to the scaled model, and blue points are the measurement locations introduced in Section 2.3. (For interpretation of the references to colour in this figure legend, the reader is referred to the Web version of this article.)

$$u_z = 0.8206 \ln(z) + 6.903 R^2 = 0.9202 \quad (1)$$

Where u_z is the along-wind mean velocity component at a height z (m s^{-1}); z is the measured height (m). The logarithmic profile showed a roughness length ($z_0 = 0.011$ m in full scale) within the range of 0.005–0.1 m, suggesting a moderately rough atmospheric boundary layer typical of grassland or farmland. The turbulence intensity in Fig. 3 (b) exhibits a decreasing trend with height. Most of the turbulent spectra at various points fall within the upper and lower boundary curves (the two blue lines recommended by VDI-VereinDeutscher (2024)), as presented in Fig. 3(a) and (d), and some points with lower values deviate from these boundary curves, indicating the limitations of the simulated wind profile near the ground level in the wind tunnel. However, other key parameters of the wind profile, including the logarithmic wind profile and turbulence intensity, were appropriately simulated in accordance with VDI-VereinDeutscher (2024). Therefore, based on the Reynolds number independence test and the airflow stability test, the atmospheric boundary layer wind profile generated at a free stream velocity of 10.0 m s^{-1} was considered acceptable to simulate the natural wind in this study.

2.4. Measurement of the airflow rate

To analyse the performance of the direct method on the measurement of the airflow rate, laterally and vertically distributed sampling points along the ventilation openings were evaluated first, followed by mesh-like sampling points composed of both lateral and vertical distributions. This process (as shown in Fig. 4) was applied to Yard Opening and Window under four wind directions. The specific distribution of measurement points and sampling levels for Yard Openings and Windows are described in detail in the following section.

2.4.1. Formula for the flow rate

The ventilation openings can be divided into multiple elementary sub-areas to capture a more detailed velocity distribution. The total airflow rate into and out of the building is then calculated as the sum of

the airflow volumes across these elementary sub-areas. The equation for multipoint measurement of the airflow rate Q is defined as follows:

$$Q = \sum_{l=1}^L \sum_{v=1}^V u_{l,v} \Delta_l \Delta_v \quad (2)$$

where Δ_l and Δ_v are the sub-areas in the lateral and vertical divisions along the opening, respectively (m^2), and l and v represent the total number of elementary sub-areas in the lateral and vertical directions; $u_{l,v}$ is the normal velocity to the corresponding elementary sub-area, which is u component at $\alpha = 0^\circ$ and 180° , and the projected u and v to the opening surface at $\alpha = 60^\circ$ and 120° , respectively ($m s^{-1}$).

The normalised airflow rate Q^* was used:

$$Q^* = \frac{Q}{A^* u_{ref}} \quad (3)$$

where u_{ref} indicates the reference airspeed ($m s^{-1}$), which is the along-wind air velocity at the scaled model height (130 mm) equal to 4.93 m s^{-1} . A^* is an effective opening area for the model with Yard Opening and Window (m^2), calculated as (Chu & Lan, 2019):

$$A^* = \frac{\sum C_{dw} A_{wi} \times \sum C_{dl} A_{lj}}{\left[(\sum C_{dw} A_{wi})^2 + (\sum C_{dl} A_{lj})^2 \right]^{0.5}} \quad (4)$$

Where A_w and A_l represent the windward and leeward opening area (m^2), and subscripts i and j represent the i th and j th opening, respectively; C_d is the discharge coefficient of the opening.

2.4.2. Levels of sampling densities under four wind directions

Based on the high spatial resolution of sampling measurements across Yard Opening and Window (working as baseline sampling densities), three levels of sampling density (Levels 3, 2, and 1) were established vertically and laterally, respectively. Levels 3, 2, and 1 progressively reduce the number of measurement points. Figs. 5 and 6 illustrate the sampling points with different levels of densities distributed vertically and laterally at Yard Opening, respectively. Sampling

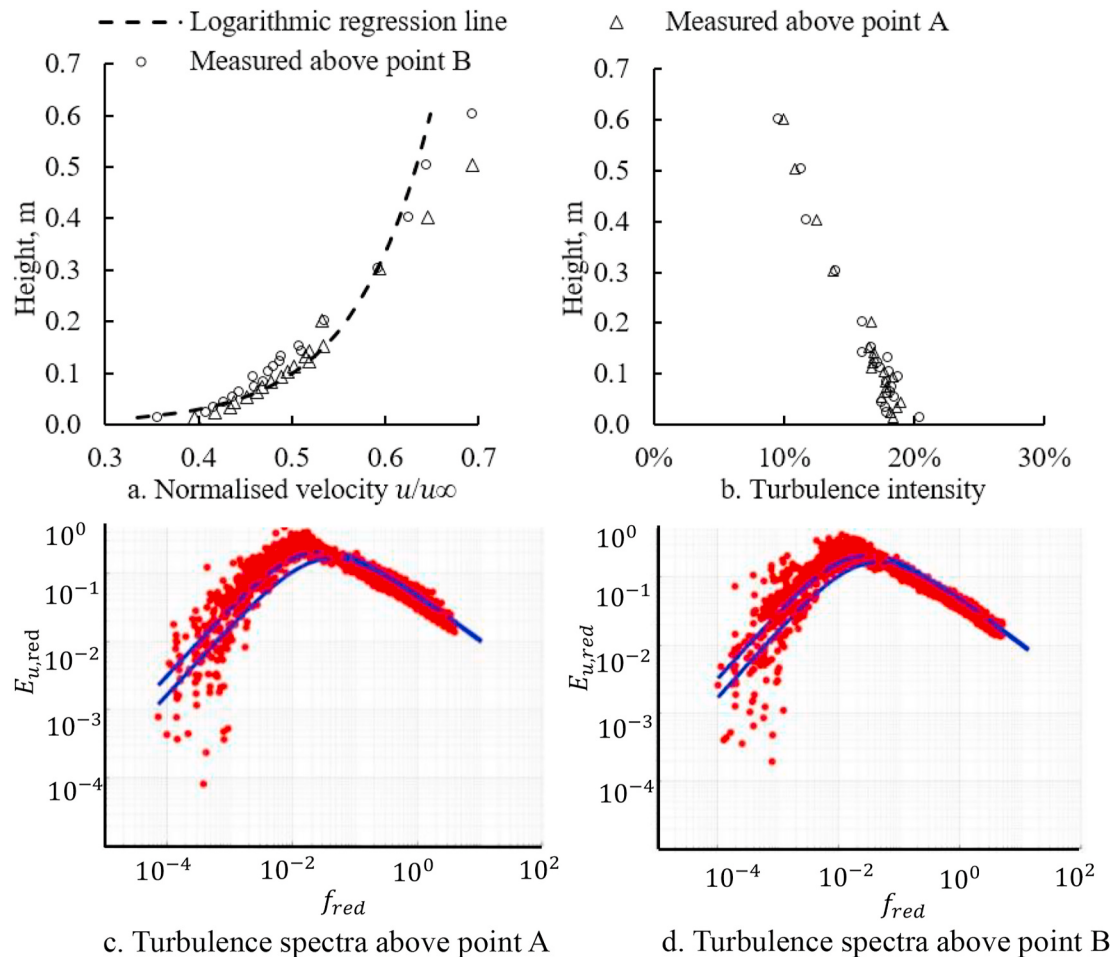


Fig. 3. Profiles of the approaching wind measured at the free stream velocity of 10.0 m s^{-1} . (a) normalised along-wind velocity u/u_∞ , (b) turbulence intensity of the u -component, (c) and (d) turbulence spectra at measurement points A and B, respectively. The red dots represent the measured spectra, and the two blue lines indicate the upper and lower boundary curves given by VDI-VereinDeutscher (2024). (For interpretation of the references to colour in this figure legend, the reader is referred to the Web version of this article.)

points across Window are shown in [appendix Fig.A1](#) and [Fig.A2](#). Those sampling densities were studied under four wind directions. Furthermore, obtaining the velocity profiles across the ventilation opening would help to better understand the performance of the sampling densities. Those Baseline sampling densities thus worked as a high spatial resolution to capture the velocity profile at the opening in each case.

2.4.3. Matrix of sampling points (mesh-like) for the airflow rate measurement

After separately evaluating the performance of vertically and laterally distributed sampling densities, suitable sampling densities in the vertical and lateral directions were selected to establish a network of multipoint measurements (mesh-like). These sampling densities varied under four wind directions, resulting in different mesh-like sampling points under each wind direction. Subsequently, to assess the accuracy of these mesh-like sampling points in measuring airflow rates, variations of mesh-like points were introduced by increasing or decreasing one-level sampling density either in the vertical or lateral direction. Those modified mesh-like sampling points were then compared with the initially determined mesh-like sampling points for each wind direction. Details of the selected sampling levels are summarised in [Table 2](#).

2.4.4. Measurement points to capture the influence of the wall effect

In order to reveal the influence of the wall effect on the quantification of the ventilation rate, a few more measurement points (Red triangles in [Fig. 7](#)) were designed in the vicinity of the two vertical edges of

Yard Opening and Window. Those points were to capture detailed airflow velocity distribution in those regions (Wall effect in the lateral direction) in order to improve the measurement accuracy. The black triangles in [Fig. 7](#) represent the sampling densities in the lateral direction without measurement to capture the wall effect, which was determined in [Section 3.3.2](#). The wall effect caused by the top and bottom edges of the openings influenced the entire airflow distribution in the vertical direction (as seen in [Sections 3.1 and 3.2](#)), so it is unrealistic to evaluate the measured airflow rate with or without the wall effect in the vertical direction. Therefore, only the wall effect caused by the vertical edges of Yard Opening and Window were discussed in this part.

2.5. Calculation of the deviations

The measurement results were quantitatively evaluated by the change ratio or the difference ratio (DR), compared to the baseline database:

$$DR = \frac{P - P_{BL}}{P_{BL}} \quad (5)$$

Where P is a placeholder for the discussed property, e.g., the measured airflow rate, normalised airflow rates, BL stands for baseline configuration, and P_{BL} stands for baseline properties. Details of the DR related to the discussed property are presented in the following sections.

The coefficient of variation (CV) was used to quantify the distribu-

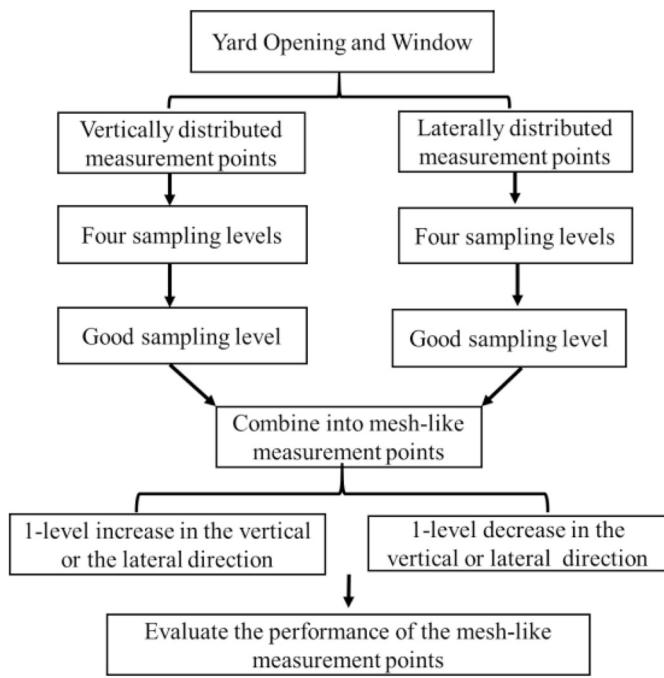


Fig. 4. Flowchart of the study evaluating the performance of the direct airflow rate measurement method.

tion of the velocity component perpendicular to the ventilation opening measured by Baseline sampling points. The CV is a statistical measure of relative dispersion or variability within a dataset, calculated as follows:

$$CV = \frac{\sigma}{\bar{u}} \times 100\% \quad (6)$$

where σ is the standard deviation of the velocity along the measurement lines. \bar{u} is the mean velocity along measurement lines ($m s^{-1}$). Generally, a lower CV indicates relatively low variability in the velocity along the measurement lines, suggesting that the velocity component distribution

is more stable and concentrated around the mean. A higher CV indicates greater variability, typically reflecting steep velocity gradients.

ANOVA (Analysis of Variance) was conducted to evaluate the significance of two factors, with a significance level set at 0.05. If $P < 0.05$, it indicates a significant difference between the two factors; conversely, if $P > 0.05$, it suggests that the difference is not statistically significant. The test statistic F reflects the between-group difference of the factors, and a greater F indicates a larger difference in the means of the groups.

3. Results and discussions

3.1. Airflow distribution at yard opening

Figs. 8 and 9 show the contours of the velocity perpendicular to the surface of Yard Opening under four wind directions, along with their average coefficient of variation (CV) for velocities distributed along the opening. For $\alpha = 0^\circ$ and 180° , similar colour zones are observed on most regions of Yard Opening in Fig. 8(a) and (d) together with a low value of CV, indicating small velocity gradients in the lateral direction under perpendicular wind directions. Instead, large velocity gradients were found for the vertical distribution at $\alpha = 0^\circ$ and 180° in Fig. 9(a) and (d), where higher air velocities (red zone) in the upper part of the opening followed by deceleration toward the top and bottom edge of the opening were observed (green or blue colour zones).

At wind direction $\alpha = 60^\circ$, the blue and the red zones (Fig. 7(b)) illustrate the coexistence of the inflow and outflow at Yard Opening, consequently leading to a high coefficient of variation ($CV = 0.872$) in the lateral direction. Differently, the vertical distribution of wind at $\alpha = 60^\circ$ shows smaller variations, observed from the similar colour zone in the vertical direction in Fig. 8(b). At $\alpha = 120^\circ$, higher air velocities were observed in the upper left corner of Comp. 1 and 2 in Figs. 8(c) and 9(c), and large velocity gradients in both the vertical and lateral directions near this region were observed, with coefficients of variation of 0.720 and 0.900, respectively. This similarity of airflow distribution in both the vertical and lateral directions at $\alpha = 120^\circ$ contrasts with the other three wind directions.

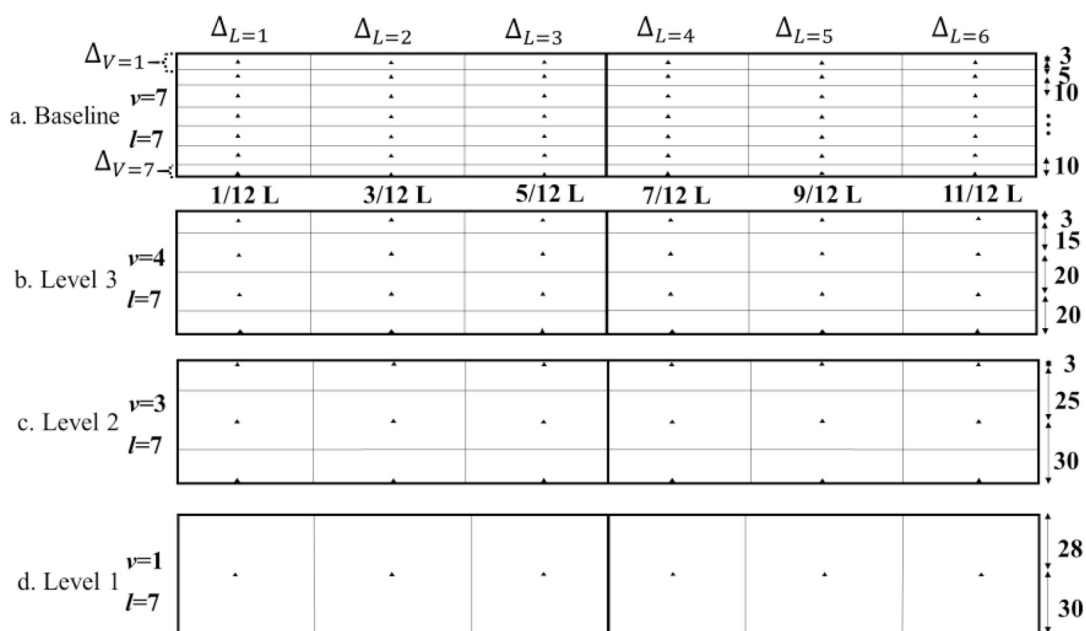


Fig. 5. Vertical distribution of measurement points across Yard Opening in six positions along the lateral direction (unit mm). Sampling levels 3, 2, and 1 were set based on Baseline. L is the lateral length of Yard Opening, which is 421 mm. v and l represent the number of sub-areas in the lateral and vertical divisions along the opening, respectively. The same for Fig. 6.

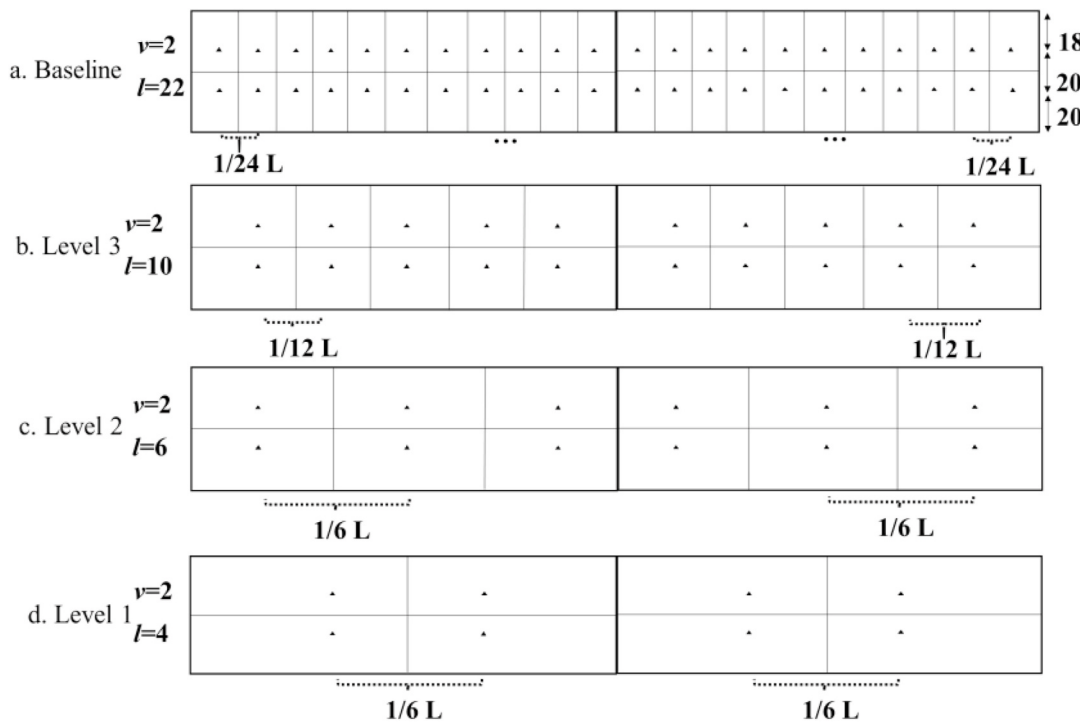


Fig. 6. Lateral distribution of measurement points across Yard Opening, with two heights of points along the vertical direction of Yard Opening (unit mm).

Table 1

Statistics values from ANOVA indicating the significance of sampling levels and wind direction on the accuracy of the measured airflow rate.

Statistics values	Factors	Yard Opening		Window	
		Dir.V	Dir.L	Dir.V	Dir.L
P	Sampling density	>0.05	>0.05	>0.05	>0.05
	Wind directions	<0.05	<0.05	<0.05	>0.05
F	Sampling density	2.77	2.81	4.03	1.71
	Wind directions	19.40	7.06	10.58	2.13

Note: Dir.V and Dir.L indicate the sampling points distributed along the vertical and the lateral directions of the opening, and the same for [Table 2](#).

3.2. Airflow distribution at window

[Figs. 10 and 11](#) show the contours of the velocity component perpendicular to the surface of Window, along with their average coefficient of variation (CV) for velocities. Window had a smaller opening size compared to Yard Opening, resulting in a completely different

airflow distribution at its opening interface.

Similar colour zones were observed at $\alpha = 0^\circ$ or 180° in [Fig. 10\(a\)](#) and (d), indicating a uniform airflow distribution in the lateral direction of Window. Under oblique wind directions ($\alpha = 60^\circ$ and 120°), unidirectional airflow with a smaller velocity gradient was observed in the lateral direction of Window ([Fig. 10\(b\)](#) and (c)), in contrast with bi-directional airflow at Yard Opening ([Fig. 8\(b\)](#) and (c)). Consequently, Window exhibited a more uniform airflow distribution in the lateral direction under oblique wind directions. This observation is indirectly consistent with findings on discharge coefficients, which show minimal impact from wind direction changes in cross-ventilation models ([Ohba et al., 2001](#)) and naturally ventilated dairy building models ([Yi, Janke, et al., 2020](#)). Moreover, the velocity profiles in the vertical direction observed under the four wind directions exhibited a peak at the centre of the Window and gradually decreased towards the edges. Their coefficients of variation (CV) in the vertical direction were higher than those in the lateral direction.

Table 2

Recommended levels to compose mesh-like sampling strategies and the performance of the modified mesh-like sampling strategies compared to the recommended one.

Opening	Wind directions	Recommended levels to compose the mesh-like sampling points		DR of the airflow rate measured through modified mesh-like sampling strategies			
		Dir.L	Dir.V	1-level rise		1-level drop	
				Dir.L	Dir.V	Dir.L	Dir.V
Yard Opening	0°	Level 2	Level 3	1.4 %	-0.6 %	8.5 %	-16.4 %
	60°	Baseline	Level 3	**	3.6 %	12.1 %	-6.6 %
	120°	Level 2	Level 2	2.0 %	1.2 %	-12.9 %	17.2 %
	180°	Level 2	Level 3	3.4 %	4.5 %	8.8 %	16.5 %
	0°	Level 1	Level 3	0.2 %	0.9 %	**	-31.0 %
	60°	Level 1	Level 3	4.0 %	-0.4 %	**	-30.6 %
Window	120°	Level 1	Level 3	0.4 %	-1.9 %	**	-9.0 %
	180°	Level 1	Level 3	-0.7 %	0.3 %	**	-6.5 %

Note: ** indicates that no data is available because the sampling levels have already reached the maximum. DR is calculated based on the recommended mesh-like sampling densities in each case. When the DR is less than 5 %, it indicates that the modified mesh-like sampling points yield a similar airflow rate to the recommended one. A 1-level rise with Dir.L indicates that the modified mesh-like sampling strategy has one higher level than the recommended one in the lateral direction, while the vertical sampling levels remained unchanged. The same applies to the other three cases.

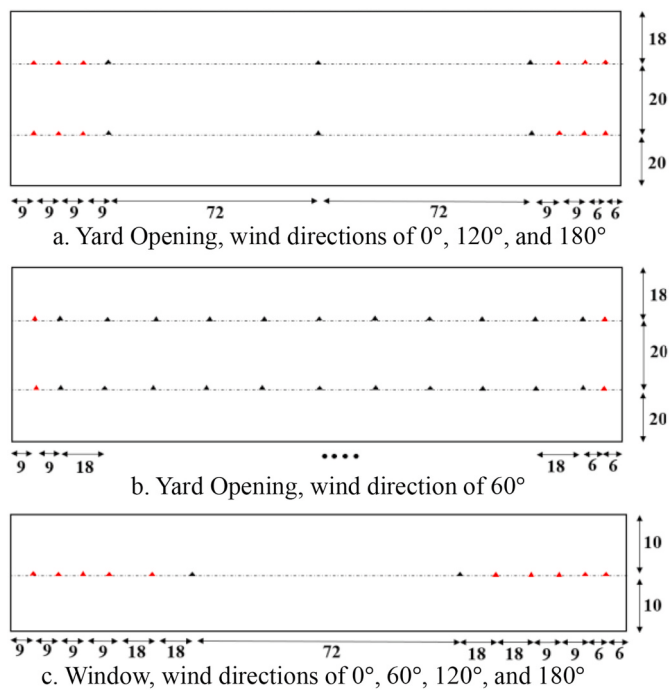


Fig. 7. Measurement points (red points) to capture the velocity distribution near the vertical edges of Yard opening and Window. Only measurement points in Comp.1 are shown, but the measurements were based on Comp.1 and 2 together. Due to different opening sizes, two rows of measurement points were placed at Yard Opening and one row at Window. Black points indicate the measurement without considering the wall effect. (For interpretation of the references to colour in this figure legend, the reader is referred to the Web version of this article.)

3.3. Influence of sampling density on the measurement of airflow rate

3.3.1. Sampling density in the vertical and lateral directions

Fig. 12 shows the change ratio (DR) of the airflow rate measured at three levels of the sampling density at Yard Opening or Window, compared to their Baseline cases, respectively. Under perpendicular wind directions ($\alpha = 0^\circ$ and 180°), Levels 2 and 1 in the vertical directions of Yard Opening caused a DR higher than 5 %, while Level 3 was less than 5 % (Fig. 12(a)). Thus, Level 3 is recommended. When considering the cases in the lateral directions, Levels 3 and 2 are acceptable, except with Level 1 with a DR of more than 5 % (Fig. 12(b)). This agrees with a study that the volume flow rate is more vulnerable to vertical positioning than to lateral positioning in dairy barns (Janke, Yi, et al., 2020). When at $\alpha = 60^\circ$, large DR was observed at all three levels in the lateral direction (because of the bi-directional airflow in Fig. 8(b)) and at Levels 2 and 1 in the vertical direction. Thereby, a dense sampling density is required in the lateral direction, and Level 3 in the vertical direction is recommended. At $\alpha = 120^\circ$, the sampling points distributed in both the vertical and the lateral directions performed well at Levels 3 and 2, while Level 1 resulted in DR exceeding 16 %.

Sampling levels at Window showed similar performance under four wind directions: DR remained below 5 % across all levels in the lateral directions. This is because the small velocity gradients in the lateral directions (Fig. 10) allowed fewer sampling points to capture the airflow rate. In the vertical direction, only Level 3 was acceptable, as its velocity profiles (a peak velocity at the center with acceleration toward the top and bottom edges, as shown in Fig. 11) require a higher sampling density for airflow rate measurements.

To quantify the influence of wind direction and sampling density on the measurement accuracy, their statistical values from the ANOVA were assessed based on DR values, as summarised in Table 1. The wind direction has a significant impact on the measured airflow rate through

Yard Opening, regardless of whether the sampling points were positioned along the vertical or lateral directions. The performance of the vertically distributed sampling points along Window was significantly affected by wind direction as well. However, the laterally distributed sampling points along Window are insignificantly affected by the wind direction, and this is consistent with the results in Fig. 12(d), where the DR values remained below 5 % across all four wind directions.

Table 1 illustrates that the sampling density had an insignificant effect on the accuracy of the measured airflow rate ($P > 0.05$). The small F value of sampling density in Table 1 suggests a small between-group difference of sampling densities, consequently leading to an insignificant effect of the sampling densities across all the studied wind directions. However, the observation that a decrease in sampling levels led to an increase in DR in Fig. 12(a–c) indicates that sampling density can significantly influence the measured results. Therefore, the influence of sampling density on the accuracy of the measured airflow rate is insignificant when considering all four wind directions together, but it still has a noticeable effect under a single direction, except for the laterally distributed sampling points at Window.

The above analysis indicates that the accuracy in airflow rate measurement through one specific setup of the sampling density and locations varied under different wind conditions. To explore the underlying reasons, Figs. 13 and 14 intuitively compare the measured values under different sampling densities, from another perspective by taking into account the velocity and the corresponding sub-areas. It is well-known that the airflow rate is calculated as the product of velocity and the corresponding sub-area of the opening, as shown in Eq. (2), and the horizontal axis represents the length of the sub-area covered by each measurement point, while the vertical length remains constant across all sampling densities and can thus be omitted. Thereby, those areas in Figs. 13 and 14 are formed by velocity curves at their sampling levels, the horizontal axis, the longitudinal axis, and the black vertical line on the right. Although the area does not represent the actual ventilation rate, it effectively illustrates differences in the measured airflow rates by highlighting variations in the area of different levels of the sampling densities.

Under perpendicular wind directions, the difference of the measured airflow arte between Level 3 or Level 2 and Baseline mainly originates from the lack of measurements in the upper part of Yard Opening, where there is a significant discrepancy in the area in Fig. 13(a) and (d). At $\alpha = 60^\circ$, the difference is mainly observed on both sides of the 30-mm-high measurement region, indicating that a lack of measurements in the upper and lower parts of the opening underestimates the airflow rate. At $\alpha = 120^\circ$, the linear variation of velocity in the vertical direction results in a small difference in area across the four sampling densities in Fig. 13(c), leading to similar measured airflow rates under different sampling levels. In Fig. 14(a) and (d), the areas of Levels 3 or 2 were small compared to Baseline, which is consistent with the difference ratio of less than 5 %. Fig. 14(b) clearly illustrates that the error in the measured airflow through Levels 3 to 1 is caused by the lack of measurement in the high-speed negative and positive velocity region at $\alpha = 60^\circ$, where there are significant differences in the areas compared to the Baseline. At $\alpha = 120^\circ$, similar areas are observed for Levels 3 and 2 compared to Baseline in Fig. 14(c) because the velocity variation in the high-speed region on one side of the opening is “linear”, allowing for a reduction in the measurement point density without causing significant errors in the areas. Figs. 13 and 14 clearly demonstrate that different sampling densities capture the airflow velocity distribution to varying degrees, highlighting the importance of evaluating the accuracy of the direct method at the Yard Opening of the studied barns.

3.3.2. Performance of the mesh-like sampling points

Mesh-like sampling strategies (the combination of the vertically and laterally distributed sampling points) can be established by the recommended sampling points in Section 3.3.1, as shown in Table 2. It should be noted that the three sampling levels in Fig. 6 did not result in a DR less

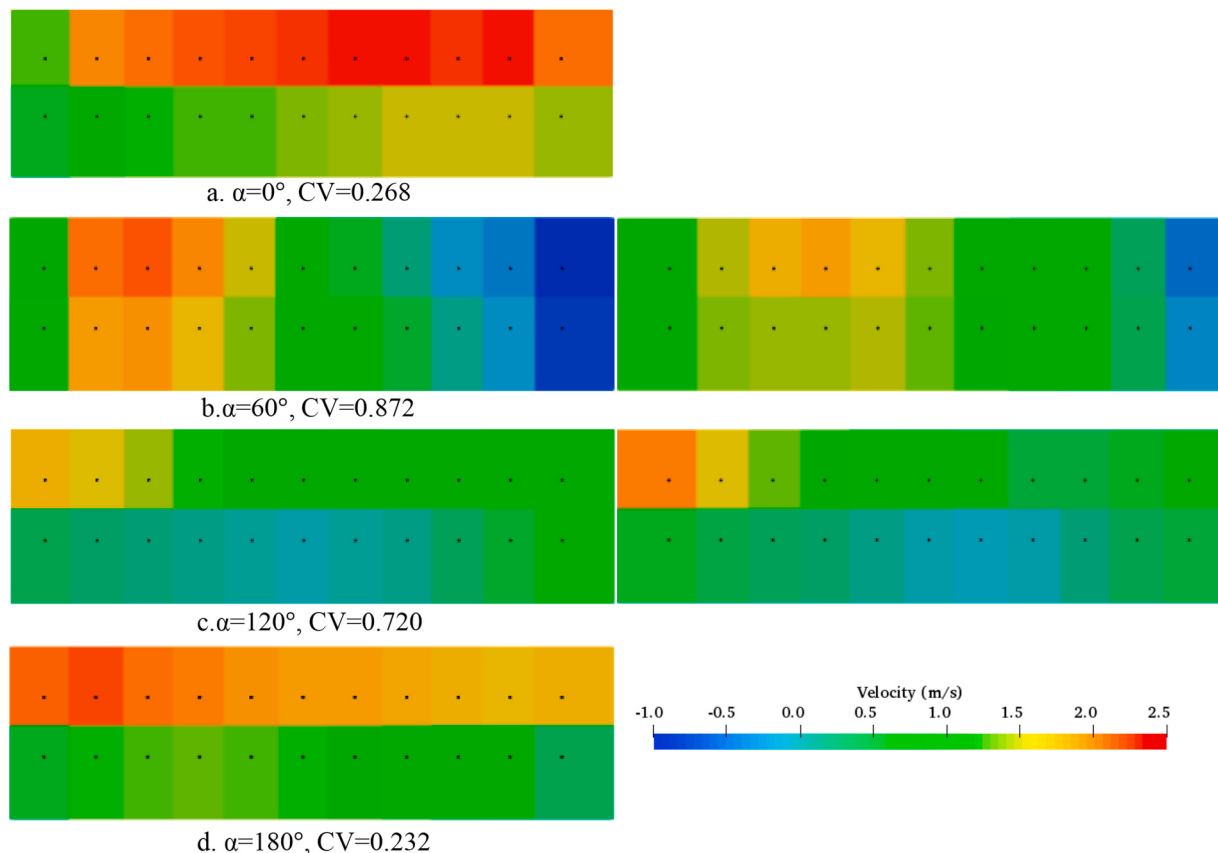


Fig. 8. Contours of wind velocity perpendicular to Yard Opening under four wind directions. The black points represent the measurement locations based on Baseline case (refer to Fig. 6a). CV represents the average coefficient of velocity variations. Under perpendicular wind directions ($\alpha = 0^\circ$ and 180°), velocities were only measured for Comp. 1 due to their symmetrical airflow distribution in Comp. 1 and Comp. 2, and the same for Figs. 9–11.

than 5 % at $\alpha = 60^\circ$. Thus, a finer sampling level with a lateral division of 9 mm (1/24 L) was deliberately added for this case, serving as a new baseline to evaluate the performance of Levels 3 to 1 and Baseline case (named Level 4 here) in the lateral direction. This process aimed to identify an acceptable sampling level $\alpha = 60^\circ$. The results showed that: the DR of Level 4, Level 3, Level 2, and Level 1 were 1.7 %, 13.9 %, 9.7 %, and 29.1 %, respectively, and consequently, Level 4 in the lateral direction is recommended. Therefore, Level 4 (the lateral direction) together with Level 3 (the vertical direction) was combined to mesh-like sampling points for Yard Opening at $\alpha = 60^\circ$.

The mesh-like sampling points with an increase or decrease of sampling density either in the vertical or the lateral direction were assessed in Table 2. Compared with the determined mesh-like sampling densities, modified sampling densities with a one-level increase either in the vertical or lateral direction resulted in a DR below 5 %, while a one-level decrease had a DR greater than 5 %. These results illustrate the reliability of the determined sampling densities under different wind directions, and an insufficient point distribution either in the vertical or the lateral directions can lead to significant errors.

Furthermore, the well-performing mesh-like sampling strategies demonstrate their feasibility for airflow rate measurement. A mesh-like sampling strategy based on a 5 (vertical) \times 4 (horizontal) grid, aligned with Levels 1 and 3 in the vertical and lateral directions, respectively, ensures good performance under all wind directions. Although the lower level in the vertical direction (Level 2) meets the measurement requirement at $\alpha = 120^\circ$, to improve the operability, Level 3 can be used. Thus, the mesh-like sampling strategy at Yard Opening based on a 4-by-6 grid with 4 points in the vertical direction and 6 points in the lateral direction (corresponding to Levels 3 and 2, respectively) is feasible under most wind directions (0° , 120° , and 180°). For wind

direction 60° , which results in noticeable bidirectional airflow in the lateral direction, a higher sampling density is needed in the lateral direction.

3.4. Influence of the wall effect on the measurement of the airflow rate

The increasing velocity near the top and bottom edges towards the centre of Yard Opening and Window (the airflow distributions in Figs. 9 and 11) suggests that the wall effect is inevitable for the entire vertical wind profile. Therefore, only the wall effect in the lateral direction was evaluated in this section. Its influence on the measured airflow rate is shown in Table 3, compared to the measured airflow rate without considering the wall effect. It can be found that all cases remained with DR less than 5 %, except for cases at $\alpha = 0^\circ$ in Yard Opening, demonstrating a small difference between the measured airflow rate with and without considering the wall effect in the lateral direction. Furthermore, Table 3 also compares the airflow rate with the wall effect with those measured through Baseline cases in the lateral direction. The measured airflow rate with the wall effect remained DR below 5 % of the whole airflow rate, and thereby, this is why the small amount of the airflow rate affected by the wall effect did not significantly influence the measured results when the measurement did not cover the wall effect region.

Furthermore, regarding the sampling points on the wall effect, some studies recommended placing the measurement points as far as possible from obstacles, as the vertical beams of the model's supporting structure and the gable wall were observed to reduce velocities near these positions (Janke, Yi, et al., 2020), which was also observed in our study. Nevertheless, those reduced velocity streams did not greatly influence the measured airflow rate. This is because the openings in naturally

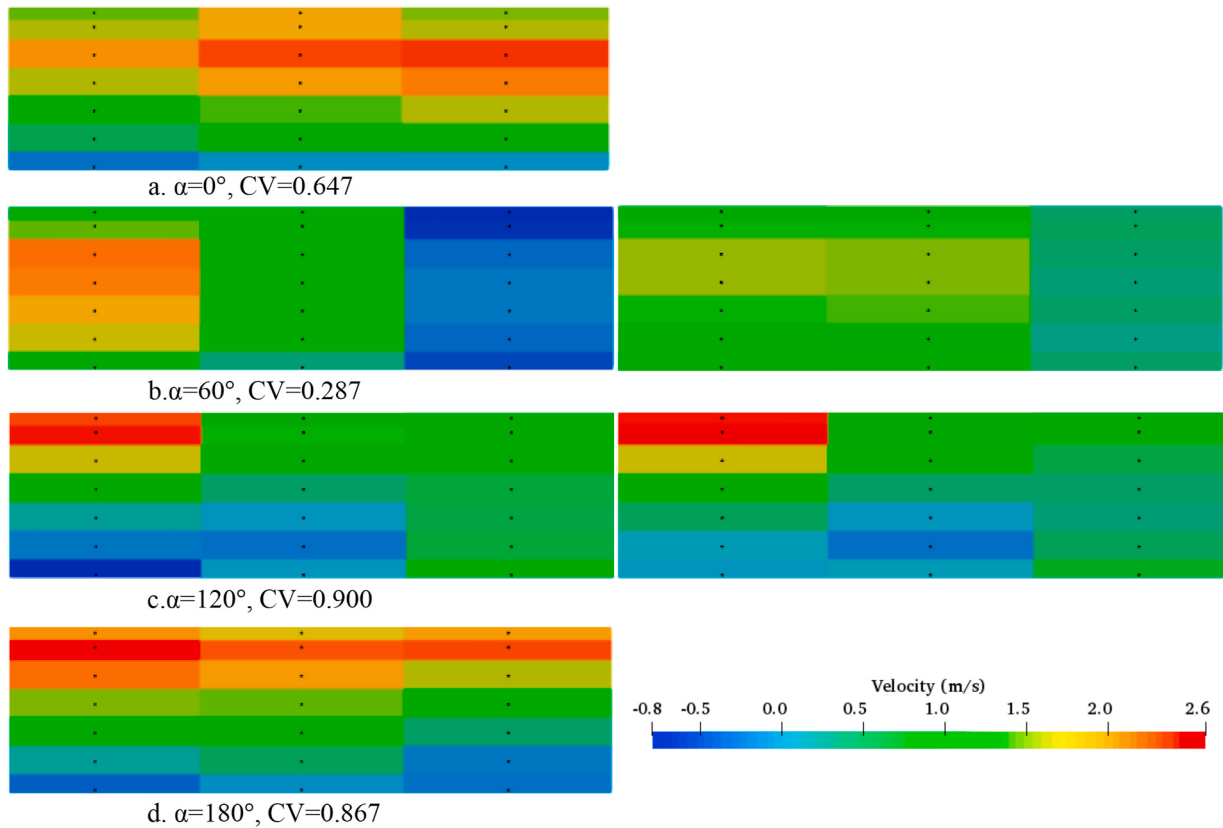


Fig. 9. Contours of wind velocity perpendicular to the opening surface at Yard Opening. The measurement points were distributed in the vertical direction (refer to Fig. 5a).

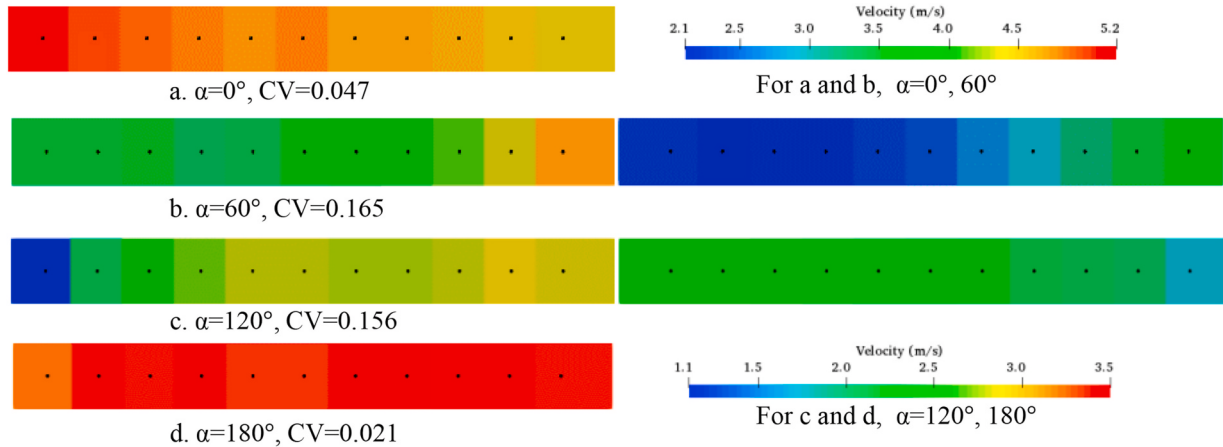


Fig. 10. Contours of wind velocity perpendicular to the opening surface of Window under four wind directions. The black points represent the measurement points distributed in the lateral direction (refer to Fig.A2).

ventilated livestock barns usually have a large lateral dimension, and there are only three vertical edges in the openings of the model. Therefore, when sampling points are properly defined in the mainstream region, their airflow rate measurements are acceptable for this opening configuration.

3.5. Comparison between Yard Opening and Window

For the studied pig barn with an outdoor yard, the indoor room and the outdoor yard are designed for different functions. As a result, the opening configurations between Yard Opening and Window generally differ in opening size. This is in contrast with conventional pig barns,

where sidewall openings are typically uniform. Therefore, this section compares the performance between Yard Opening and Window.

3.5.1. Airflow distribution between Yard Opening and Window

Two types of airflow distribution in the vertical direction were observed at Yard Opening and Window and they were 1) acceleration towards higher positions of Yard Opening (Figs. 9), and 2) a peak velocity at the centre of Window (Fig. 11). Those two velocity profiles were found at the conventional livestock barns as well: 1) A maximum velocity towards the top of the opening was observed at openings directly connected to the roof of dairy barns (Janke, Caiazzo, et al., 2020; Janke, Yi et al., 2020). These barns typically have a high side-wall opening

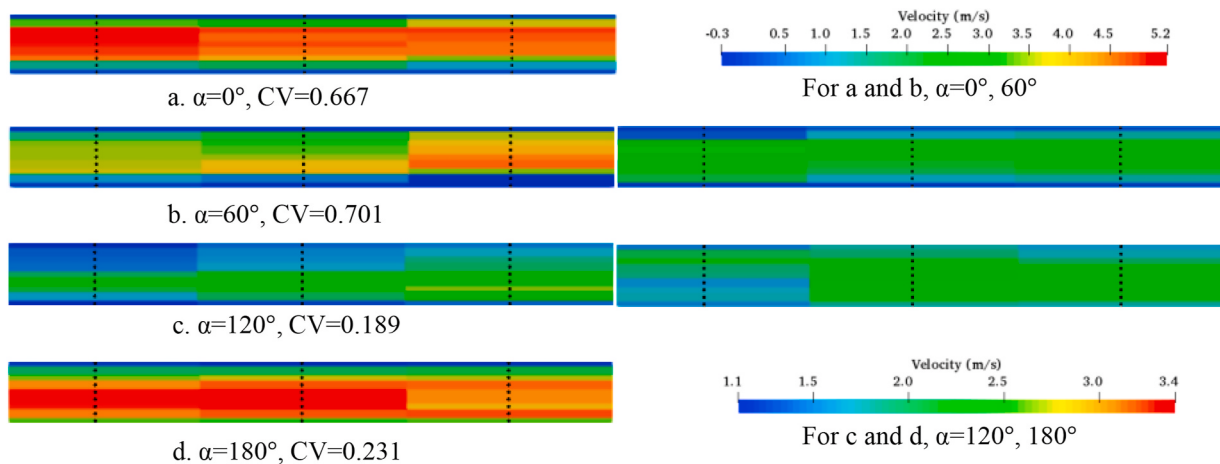


Fig. 11. Contours of wind velocity perpendicular to the opening surface of Window under four wind directions. The black points represent the measurement points distributed in the vertical direction (refer to Fig.A1).

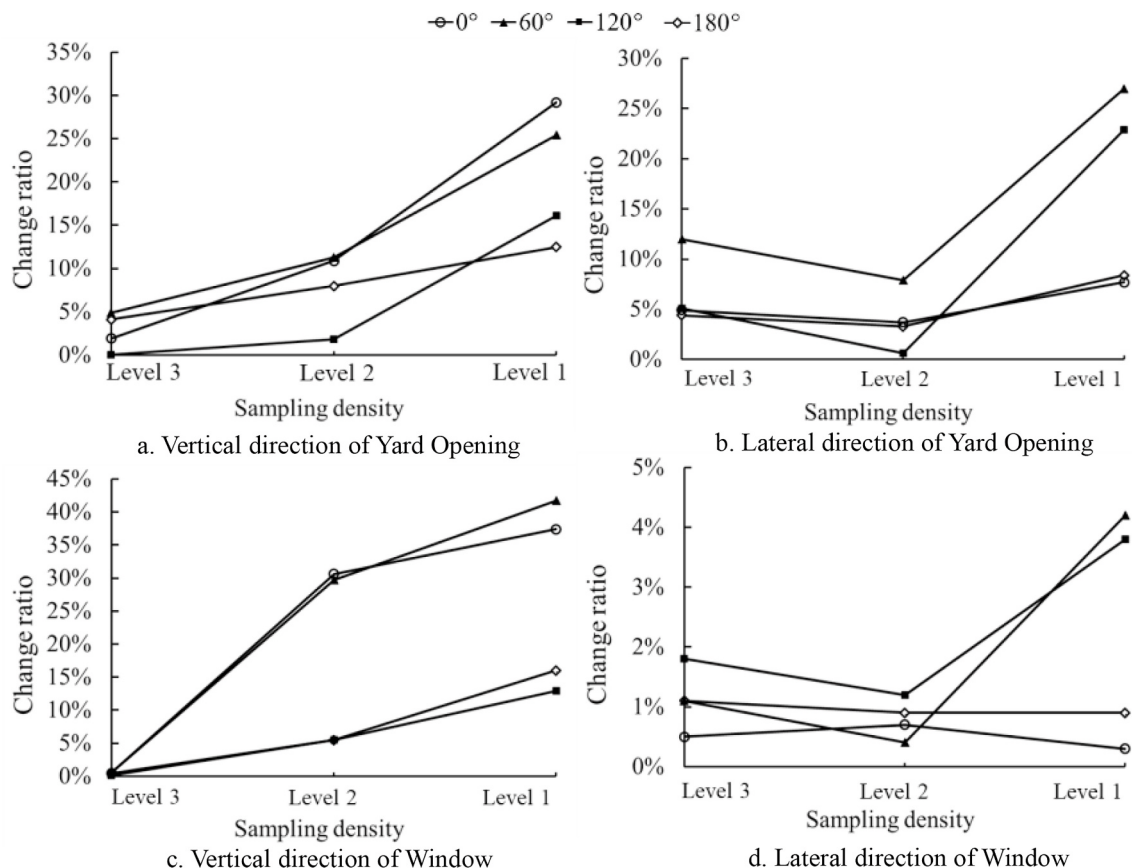


Fig. 12. Change ratio of the airflow rate measured at different sampling levels compared with baseline cases in the vertical and the lateral directions of Yard Opening and Window.

ratio, e.g., dairy stables (Ngwabie et al., 2009; Saha et al., 2013), and are representative of the northern and eastern regions of Germany (Fiedler et al., 2014). This airflow distribution can be explained: Its larger vertical dimension leads to a weakened wall effect in regions farther from the top and bottom edges, and the sloped eaves tend to guide airflow upwards through the opening, allowing more space for airflow to develop in the vertical direction (Ikeguchi & Okushima, 2001; Yi, Janke, et al., 2020). 2) A peak velocity at the centre of the opening was frequently reported in small barns with small opening ratios (De Vogeeler et al., 2016, 2017). These barns usually have openings that are

not directly connected to the roof but are instead separated by a wall above the opening, or they rely primarily on ridge ventilation. This is a typical design in parts of southern Europe or used for naturally ventilated pig barns, usually with a small opening ratio (Janke, Yi, et al., 2020). For example, in a naturally ventilated pig barn in northern Italy, there are 0.9 m high openings on the sidewalls and 0.85 m high roof openings (Bovo et al., 2022). In a naturally ventilated dairy barn in southern Italy, the total width of the ridge opening is 0.6 m, and the vertical sidewalls have openings accounting for 30 % of their surface area (De Masi et al., 2021). Airflow distributions at Window in the

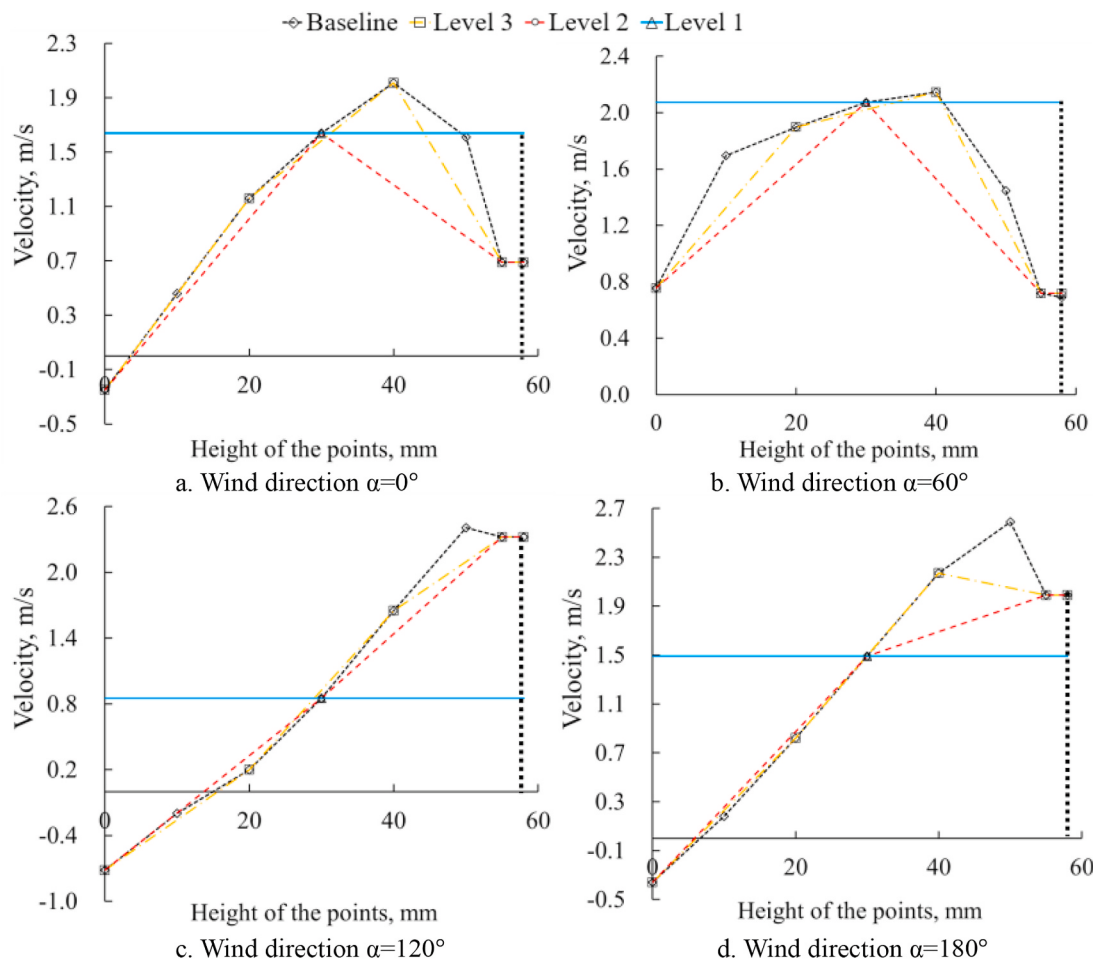


Fig. 13. Velocity distribution in the vertical direction measured through different levels of the sampling densities (Measurement lines were 180 mm to the Mid-Partition wall in Comp.1). The area defined by the velocity curves, x-axis, longitudinal axes, and the black line on the right side, and the discrepancies between these areas intuitively highlight the difference in the measured airflow rate at different sampling levels and the same for Fig. 14.

vertical direction resembled the parabolic velocity profiles observed at openings of naturally ventilated pig houses with side openings of 0.5 m × 3.0 m (De Vogeeler et al., 2017) and 4.5 m × 0.5 m (Van Overbeke et al., 2015), and a naturally ventilated air opening of 0.6 m × 0.6 m (Özcan et al., 2009). Therefore, the similar airflow distribution observed in openings with relatively short vertical dimensions can be explained by the strong wall effect in the vertical direction, which constrains airflow development and thus leads to such airflow distributions at those types of openings.

Therefore, considering the relationship between the openings and the eaves of the barn, the sampling density and location used in this study can be reasonably applied to these two types of openings in conventional naturally ventilated livestock buildings, due to the similar airflow distribution patterns at Yard Opening and Window compared to those found in conventional barns.

3.5.2. Measured airflow rate between Yard Opening and Window

Based on those determined mesh-like sampling points, the airflow rate through Yard Opening and Window under four wind directions can be obtained, and the normalised airflow rate is shown in Table 4. DR greater than 5 % was observed at $\alpha = 0^\circ$, because the relatively large discrepancy in the measured airflow rate at Yard Opening and Window, resulted from a necessary 2–3 mm displacement of the LDA measurement position from the exact opening location at Window to avoid laser reflection and occlusion caused by the roof sheet. However, DR less than 10 % is acceptable, and this airflow rate at $\alpha = 0^\circ$ was used for analysis.

Yard Opening functions as a windward surface at $\alpha = 0^\circ$, while as a

leeward opening at $\alpha = 180^\circ$, consequently resulting in different airflow rates under perpendicular wind directions. In this study, Q^*_{Average} at $\alpha = 0^\circ$ and 180° are close to Q^* of 0.6210 and 0.4891 for a naturally ventilated dairy barn with two opening ratios (opening area/(opening area + sidewall area)) of 55.9 % and 18.6 % (Yi et al., 2018), respectively, under perpendicular wind direction. This similar airflow rate between the barn with an outdoor yard and conventional livestock barns with large and small opening ratios reflects the different influences of Yard Opening and Window on the ventilation. Furthermore, Q^*_{Average} at $\alpha = 60^\circ$ accounts for 58.2 % of that at $\alpha = 0^\circ$, and Q^*_{Average} 63.1 % at $\alpha = 120^\circ$ of that at $\alpha = 180^\circ$, respectively. This result does not align with the cosine law typically observed in civil buildings (Chu et al., 2011) and livestock buildings (Yi et al., 2019) where an approximate 50 % ($\cos 60^\circ = 0.5$) reduction in the airflow rate is expected at a wind direction of 60° compared to perpendicular wind directions. This discrepancy may be attributed to the 20-mm-long protrusion of the Mid-Partition wall between Comp. 1 and 2, which could lead to higher airflow under oblique wind directions. Further study is needed to find out the exact cause. The airflow rates under four wind directions illustrate that the orientation of the pig barn is crucial for maintaining proper ventilation.

3.6. Research limitations and perspectives

One specific mesh-like sampling strategy was determined for Yard Opening under three wind directions (0° , 120° , and 180°), except for wind direction 60° due to the bidirectional airflow. However, a 60° gap in the wind direction might be too large to accurately distinguish the

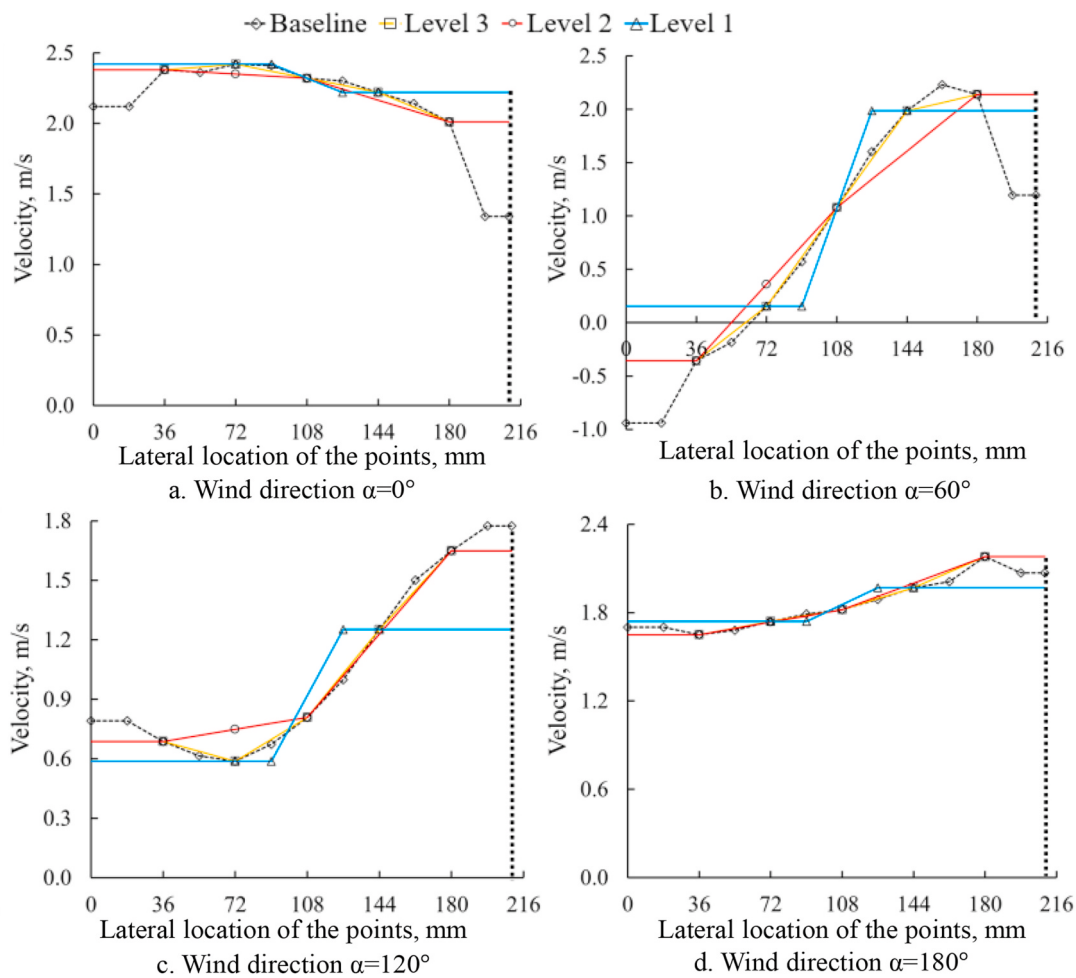


Fig. 14. Velocity distribution in the lateral direction measured through different levels of the sampling densities (Measurement lines were 50 mm high above the bottom edge of Yard Opening).

Table 3

Difference ratio (DR) of the measured airflow rate considering the wall effect, compared to the Baseline levels and sampling densities without considering wall effect.

Wind directions	Opening	DR compared to Baseline sampling levels	DR compared to determined sampling levels
0 °	Yard Opening	-3.2 %	-6.7 %
	Window	-0.9 %	-0.9 %
60 °	Yard Opening	-2.0 %	0.9 %
	Window	0.1 %	0.5 %
120 °	Yard Opening	3.9 %	4.6 %
	Window	-2.5 %	-3.6 %
180 °	Yard Opening	2.4 %	0.2 %
	Window	-0.6 %	-1.4 %

Note: The results are based on Comp. 1 and 2 for 60 ° and 120 °, and only Comp. 2 for 0 ° and 180 ° since their symmetric airflow distributions between two compartments under perpendicular wind directions.

critical wind direction when the bidirectional airflow significantly affects the performance of this specific mesh-like sampling strategy. Therefore, further studies should be conducted under more detailed wind directions to identify the range of wind directions for which this

Table 4

Statistical results of the measured airflow rate through Yard Opening and Window.

Wind direction (α)	$Q^*_{\text{Yard Opening}}$	Q^*_{Window}	Q^*_{Average}	$DR_{\text{Yard Opening-Q*Average}}$
0 °	0.690	0.563	0.627	8.65 %
60 °	0.376	0.355	0.365	2.91 %
120 °	0.305	0.313	0.308	1.24 %
180 °	0.511	0.465	0.488	4.80 %

Note: $Q^*_{\text{Yard Opening}}$ and Q^*_{Window} represent the normalised airflow rates measured at Yard Opening and Window, respectively. Q^*_{Average} refers to the airflow rate averaged from the measured rates at Yard Opening and Window. $DR_{\text{Yard Opening-Q*Average}}$ is the difference ratio of $Q^*_{\text{Yard Opening}}$ with Q^*_{Average} as a baseline.

mesh-like sampling strategy performs well. Moreover, the good performance of the sampling strategies determined in this study makes them easily applicable to wind tunnel experiments and steady-state CFD simulations due to their stable environmental conditions. However, the constantly fluctuating natural wind and the buoyancy effect were not considered in the study, which might lead to more complex airflow distribution. Furthermore, mesh-like sampling points, which typically involve a large number of measurements, increase the cost of the experiment and also would disturb the airflow velocity distribution. Therefore, further studies are needed to validate these findings under actual farm conditions and then to simplify the sampling strategy in order to enhance the feasibility of the direct method for airflow rate

measurements in the barn with an outdoor yard.

4. Conclusion

The effect of the sampling density and location on the airflow rate measurement in a naturally ventilated pig barn with an outdoor exercise yard was studied based on a large atmospheric boundary layer wind tunnel. Different sampling densities and locations were used at Yard Opening and Window of the model under four wind directions. The following conclusions have been made:

- 1) To accurately measure the airflow rate using the direct method, a mesh-like sampling strategy is recommended for the studied barn: a 4-by-6 grid (4 points in the vertical direction and 6 points in the lateral direction) at Yard Opening, and a 5-by-4 grid (5 points vertically and 4 points horizontally) at Window.
- 2) An appropriate mesh-like sampling strategy for Window can ensure an accurate airflow rate (a change ratio less than 5 %) under different wind directions. The mesh-like sampling strategy for Yard Opening performs well under wind directions of $\alpha = 0^\circ$, 120° , and 180° . As for $\alpha = 60^\circ$, a higher sampling density is needed because of the bidirectional airflow in the lateral direction of Yard Opening.
- 3) For both Yard Opening and Window, the airflow rate influenced by the vertical sides of the openings accounts for less than 5 % of the overall airflow rate and can therefore be disregarded when setting up measurement points. However, the wall effects from the top and bottom edges of the openings significantly affect the entire velocity profile and should be taken into consideration.
- 4) Wind direction had a significant impact on the measured airflow rate and airflow velocity distribution through Yard Opening, compared to that through Window. The airflow velocity distributions at both Yard Opening and Window were similar to those observed at openings of conventional barns without an outdoor yard, indicating the potential for adopting a similar sampling point arrangement.

Appendix

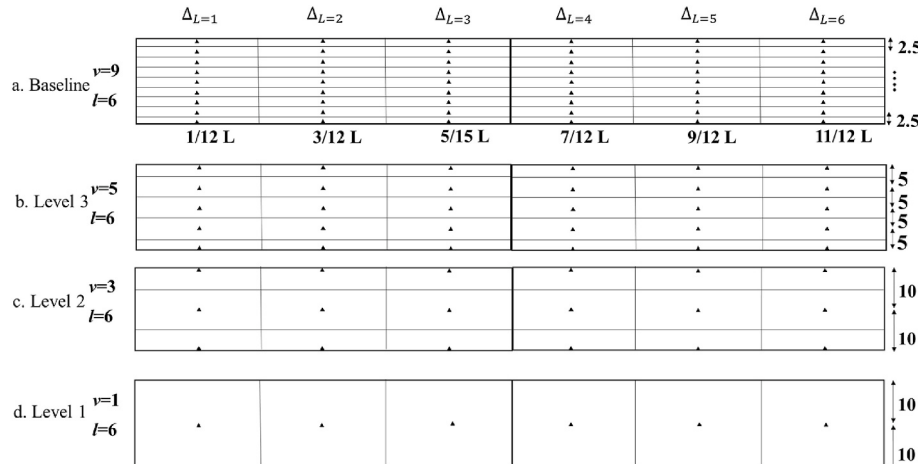


Fig. A1. Vertical distribution of measurement points across Window in six positions along lateral direction of the opening (unit mm). Sampling levels 3, 2, and 1 were set based on Baseline. L is the lateral length of Window, which is 421 mm. v and l represent the number of surfaces in the lateral and vertical divisions along the opening, respectively. The same for Fig.A2.

CRediT authorship contribution statement

Xuefei Wu: Writing – original draft, Methodology, Investigation, Formal analysis, Data curation, Conceptualization. **Sabrina Hempel:** Writing – review & editing, Conceptualization. **David Janke:** Writing – review & editing, Conceptualization. **Barbara Amon:** Writing – review & editing, Conceptualization. **Guoqiang Zhang:** Writing – review & editing, Conceptualization. **Jürgen Zentek:** Writing – review & editing, Supervision. **Thomas Amon:** Writing – review & editing, Supervision, Conceptualization. **Qianying Yi:** Writing – review & editing, Supervision, Project administration, Funding acquisition, Conceptualization.

Declaration of competing interest

The authors declare that they have no known competing financial interests or personal relationships that could have appeared to influence the work reported in this paper.

Acknowledgements

We gratefully acknowledge the financial support from the research project funded by Deutsche Forschungsgemeinschaft (DFG, German Research Foundation), Grant Number 467000790. The authors also thank technician Andreas Reinhardt and engineer Lars Thormann at ATB for their work in experiment operations and suggestions.

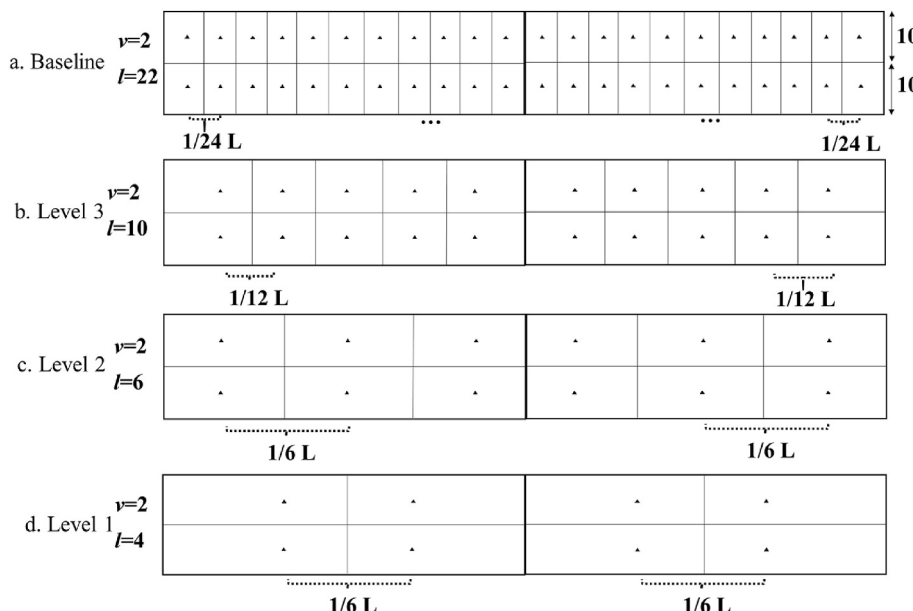


Fig. A2. Lateral distribution of measurement points across Window, with one height of points along the vertical direction of Yard Opening (unit mm).

Data availability

Data will be made available on request.

References

- Andersen, H. M.-L., Kongsted, A. G., & Jakobsen, M. (2020). Pig elimination behavior—a review. *Applied Animal Behaviour Science*, 222, Article 104888. <https://doi.org/10.1016/j.applanim.2019.104888>
- Bovo, M., Santolini, E., Barbaresi, A., Tassinari, P., & Torreggiani, D. (2022). Assessment of geometrical and seasonal effects on the natural ventilation of a pig barn using CFD simulations. *Computers and Electronics in Agriculture*, 193, Article 106652. <https://doi.org/10.1016/j.compag.2021.106652>
- Caio, M., Yi, Q., Wang, K., Li, J., & Wang, X. (2023). Predicting ventilation rate in a naturally ventilated dairy barn in wind-forced conditions using machine learning techniques. *Agriculture*, 13(4), 837. <https://doi.org/10.3390/agriculture13040837>
- Cheng, X.-X., Zhao, L., Ge, Y.-J., Dong, J., & Peng, Y. (2024). Full-scale/model test comparisons to validate the traditional atmospheric boundary layer wind tunnel tests: Literature review and personal perspectives. *Applied Sciences*, 14(2), 782. <https://doi.org/10.3390/app14020782>
- Chu, C. R., Chen, R.-H., & Chen, J.-W. (2011). A laboratory experiment of shear-induced natural ventilation. *Energy and Buildings*, 43(10), 2631–2637. <https://doi.org/10.1016/j.enbuild.2011.06.014>
- Chu, C.-R., & Lan, T.-W. (2019). Effectiveness of ridge vent to wind-driven natural ventilation in monoslope multi-span greenhouses. *Biosystems Engineering*, 186, 279–292. <https://doi.org/10.1016/j.biosystemseng.2019.08.006>
- De Masi, R. F., Ruggiero, S., Tariello, F., & Vanoli, G. P. (2021). Passive envelope solutions to aid design of sustainable livestock buildings in Mediterranean climate. *Journal of Cleaner Production*, 311, Article 127444. <https://doi.org/10.1016/j.jclepro.2021.127444>
- De Vogeeler, G., Pieters, J. G., Van Overbeke, P., & Demeyer, P. (2017). Effect of sampling density on the reliability of airflow rate measurements in a naturally ventilated animal mock-up building. *Energy and Buildings*, 152, 313–322. <https://doi.org/10.1016/j.enbuild.2017.07.032>
- De Vogeeler, G., Van Overbeke, P., Brusselman, E., Mendes, L. B., Pieters, J. G., & Demeyer, P. (2016). Assessing airflow rates of a naturally ventilated test facility using a fast and simple algorithm supported by local air velocity measurements. *Building and Environment*, 104, 198–207. <https://doi.org/10.1016/j.buildenv.2016.05.006>
- Fiedler, M., Saha, C. K., Ammon, C., Berg, W., Loebis, C., Sanftleben, P., & Amon, T. (2014). Spatial distribution of air flow and CO₂ concentration in a naturally ventilated dairy building. *Environmental Engineering and Management Journal*, 13(9), 2193–2200. <https://doi.org/10.30638/eemj.2014.244>
- Ikeguchi, A., & Okushima, L. (2001). Airflow patterns related to polluted air dispersion in open freestall dairy houses with different roof shapes. *Transactions of the ASAE*, 44 (6). <https://doi.org/10.13031/2013.7016>
- Janke, D., Caiazzo, A., Ahmed, N., Alia, N., Knoth, O., Moreau, B., Wilbrandt, U., Willink, D., Amon, T., & John, V. (2020). On the feasibility of using open source solvers for the simulation of a turbulent air flow in a dairy barn. *Computers and Electronics in Agriculture*, 175, Article 105546. <https://doi.org/10.1016/j.compag.2020.105546>
- Janke, D., Willink, D., Ammon, C., Hempel, S., Schrade, S., Demeyer, P., Hartung, E., Amon, B., Ogink, N., & Amon, T. (2020). Calculation of ventilation rates and ammonia emissions: Comparison of sampling strategies for a naturally ventilated dairy barn. *Biosystems Engineering*, 198, 15–30. <https://doi.org/10.1016/j.biosystemseng.2020.07.011>
- Janke, D., Yi, Q., Thormann, L., Hempel, S., Amon, B., Nosek, Š., van Overbeke, P., & Amon, T. (2020). Direct measurements of the volume flow rate and emissions in a large naturally ventilated building. *Sensors*, 20(21), 6223. <https://doi.org/10.3390/s20216223>
- Joo, H. S., Ndegwa, P. M., Heber, A. J., Bogan, B. W., Ni, J.-Q., Cortus, E. L., & Ramirez-Dorronsoro, J. C. (2014). A direct method of measuring gaseous emissions from naturally ventilated dairy barns. *Atmospheric Environment*, 86, 176–186. <https://doi.org/10.1016/j.atmosenv.2013.12.030>
- Kiwan, A., Berg, W., Fiedler, M., Ammon, C., Gläser, M., Müller, H.-J., & Brunsch, R. (2013). Air exchange rate measurements in naturally ventilated dairy buildings using the tracer gas decay method with 85Kr, compared to CO₂ mass balance and discharge coefficient methods. *Biosystems Engineering*, 116(3), 286–296. <https://doi.org/10.1016/j.biosystemseng.2012.11.011>
- Lee, I. B., Kang, C., Lee, S., Kim, G., Heo, J., & Sase, S. (2004). Development of vertical wind and turbulence profiles of wind tunnel boundary layers. *Transactions of the ASAE*, 47(5), 1717–1726. <https://doi.org/10.13031/2013.17614>
- Ngawib, N. M., Jeppsson, K.-H., Nimmermark, S., Svensson, C., & Gustafsson, G. (2009). Multi-location measurements of greenhouse gases and emission rates of methane and ammonia from a naturally-ventilated barn for dairy cows. *Biosystems Engineering*, 103(1), 68–77. <https://doi.org/10.1016/j.biosystemseng.2009.02.004>
- Nosek, Š., Kluková, Z., Jakubcová, M., Yi, Q., Janke, D., Demeyer, P., & Jaňour, Z. (2020). The impact of atmospheric boundary layer, opening configuration and presence of animals on the ventilation of a cattle barn. *Journal of Wind Engineering and Industrial Aerodynamics*, 201, Article 104185. <https://doi.org/10.1016/j.jweia.2020.104185>
- Ohba, M., Irie, K., & Kurabuchi, T. (2001). Study on airflow characteristics inside and outside a cross-ventilation model, and ventilation flow rates using wind tunnel experiments. *Journal of Wind Engineering and Industrial Aerodynamics*, 89(14–15), 1513–1524. [https://doi.org/10.1016/S0167-6105\(01\)00130-1](https://doi.org/10.1016/S0167-6105(01)00130-1)
- Özcan, S. E., Vranken, E., & Berckmans, D. (2009). Measuring ventilation rate through naturally ventilated air openings by introducing heat flux. *Building and Environment*, 44(1), 27–33. <https://doi.org/10.1016/j.buildenv.2008.01.011>
- Saha, C. K., Ammon, C., Berg, W., Loebis, C., Fiedler, M., Brunsch, R., & von Bobrutzki, K. (2013). The effect of external wind speed and direction on sampling point concentrations, air change rate and emissions from a naturally ventilated dairy building. *Biosystems Engineering*, 114(3), 267–278. <https://doi.org/10.1016/j.biosystemseng.2012.12.002>
- Samer, M., Ammon, C., Loebis, C., Fiedler, M., Berg, W., Sanftleben, P., & Brunsch, R. (2012). Moisture balance and tracer gas technique for ventilation rates measurement and greenhouse gases and ammonia emissions quantification in naturally ventilated buildings. *Building and Environment*, 50, 10–20. <https://doi.org/10.1016/j.buildenv.2011.10.008>
- Samer, M., Loebis, C., Fiedler, M., Ammon, C., Berg, W., Sanftleben, P., & Brunsch, R. (2011). Heat balance and tracer gas technique for airflow rates measurement and

- gaseous emissions quantification in naturally ventilated livestock buildings. *Energy and Buildings*, 43(12), 3718–3728. <https://doi.org/10.1016/j.enbuild.2011.10.008>
- Seedorf, J., Hartung, J., Schröder, M., Linkert, K. H., Pedersen, S., Takai, H., Johnsen, J. O., Metz, J. H. M., Groot Koerkamp, P. W. G., Uenk, G. H., Phillips, V. R., Holden, M. R., Sneath, R. W., Short, J. L. L., White, R. P., & Wathes, C. M. (1998). A survey of ventilation rates in livestock buildings in northern Europe. *Journal of Agricultural Engineering Research*, 70(1), 39–47. <https://doi.org/10.1006/jaer.1997.0274>
- Van Overbeke, P., De Vogeeler, G., Brusselman, E., Pieters, J. G., & Demeyer, P. (2015). Development of a reference method for airflow rate measurements through rectangular vents towards application in naturally ventilated animal houses: Part 3: Application in a test facility in the open. *Computers and Electronics in Agriculture*, 115, 97–107. <https://doi.org/10.1016/j.compag.2015.05.009>
- Van Overbeke, P., De Vogeeler, G., Pieters, J. G., & Demeyer, P. (2014). Development of a reference method for airflow rate measurements through rectangular vents towards application in naturally ventilated animal houses: Part 2: Automated 3D approach. *Computers and Electronics in Agriculture*, 106, 20–30. <https://doi.org/10.1016/j.compag.2014.05.004>
- Van Overbeke, P., Pieters, J. G., De Vogeeler, G., & Demeyer, P. (2014). Development of a reference method for airflow rate measurements through rectangular vents towards application in naturally ventilated animal houses: Part 1: Manual 2D approach. *Computers and Electronics in Agriculture*, 106(2014), 31–41.
- VDI-Verein Deutscher. (2024). *Environmental meteorology - physical modelling of flow and dispersion processes in the atmospheric boundary layer - application of wind tunnels*, VDI-standard: Vdi (p. 202). Berlin, German: Deutsches Institut für Normung.
- Wang, X., Ndegwa, P. M., Joo, H., Neerackal, G. M., Stöckle, C. O., Liu, H., & Harrison, J. H. (2016). Indirect method versus direct method for measuring ventilation rates in naturally ventilated dairy houses. *Biosystems Engineering*, 144, 13–25. <https://doi.org/10.1016/j.biosystemseng.2016.01.010>
- Wu, X., Janke, D., Hempel, S., Zentek, J., Amon, B., Amon, T., & Yi, Q. (2025). Wind tunnel study on effect of wind directions on ventilation inside a naturally ventilated pig barn with an outdoor yard. *Biosystems Engineering*, 253, Article 104123. <https://doi.org/10.1016/j.biosystemseng.2025.104123>
- Yi, Q., Janke, D., Thormann, L., Zhang, G., Amon, B., Hempel, S., Nosek, Š., Hartung, E., & Amon, T. (2020). Airflow characteristics downwind a naturally ventilated pig building with a roofed outdoor exercise yard and implications on pollutant distribution. *Applied Sciences*, 10(14), 4931. <https://doi.org/10.3390/app10144931>
- Yi, Q., Wang, X., Zhang, G., Li, H., Janke, D., & Amon, T. (2019). Assessing effects of wind speed and wind direction on discharge coefficient of sidewall opening in a dairy building model – a numerical study. *Computers and Electronics in Agriculture*, 162, 235–245. <https://doi.org/10.1016/j.compag.2019.04.016>
- Yi, Q., Zhang, G., König, M., Janke, D., Hempel, S., & Amon, T. (2018). Investigation of discharge coefficient for wind-driven naturally ventilated dairy barns. *Energy and Buildings*, 165, 132–140. <https://doi.org/10.1016/j.enbuild.2018.01.038>
- Yi, Q., Zhang, G., Li, H., Wang, X., Janke, D., Amon, B., Hempel, S., & Amon, T. (2020). Estimation of opening discharge coefficient of naturally ventilated dairy buildings by response surface methodology. *Computers and Electronics in Agriculture*, 169, Article 105224. <https://doi.org/10.1016/j.compag.2020.105224>